

## Low-lying magnetic excitations in Ni<sub>3</sub>Al and their suppression by a magnetic field

Anita Semwal and S. N. Kaul\*

*School of Physics, University of Hyderabad, Central University P.O., Hyderabad 500 046, Andhra Pradesh, India*

(Received 3 May 1999; revised manuscript received 21 July 1999)

Results of high-resolution magnetization ( $M$ ) measurements performed on well-characterized polycrystalline Ni<sub>3</sub>Al sample over wide ranges of temperature and external magnetic field are presented and discussed in the light of existing theoretical models. Contrary to the earlier claims that either Stoner single-particle excitations or nonpropagating spin fluctuations solely determine the temperature dependence of spontaneous magnetization  $M(T,0)$ , at low temperatures, we find that propagating transverse spin-density fluctuations (spin waves) almost entirely account for the thermal demagnetization of both  $M(T,0)$  and ‘‘in-field’’ magnetization  $M(T,H)$ , at temperatures  $T \lesssim 0.28T_C$  ( $T_C$ =Curie point). The spin-wave stiffness possesses a field-independent value of  $69.6(14)$  meV  $\text{\AA}^2$  which conforms well with those determined earlier from small-angle and inelastic neutron-scattering experiments. In the temperature range  $0.32T_C \lesssim T \lesssim 0.92T_C$ , enhanced nonpropagating spin-density fluctuations (SF) give a contribution to  $M(T,0)$  and  $M(T,H)$  that completely overshadows the one arising from spin waves. In accordance with the predictions of a modified spin-fluctuation theory, proposed by the authors recently, the thermally excited SF’s get strongly suppressed by magnetic field  $H$  while the zero-point SF’s are relatively insensitive to  $H$ . [S0163-1829(99)01142-X]

### I. INTRODUCTION

Out of the intermetallic compounds that exhibit weak itinerant-electron ferromagnetism, ordered (cubic  $L1_2$  crystal structure) Ni<sub>3</sub>Al has captured maximum experimental and theoretical attention during the past three decades, and yet certain aspects of magnetism in this compound have eluded a complete understanding so far. One such aspect pertains to the nature of low-lying magnetic excitations. Magnetic properties of Ni<sub>3</sub>Al have been extensively studied<sup>1–11</sup> and the results discussed in the light of either Stoner-Wohlfarth<sup>1–8,12,13</sup> model or the spin fluctuation model.<sup>9–23</sup> On the one hand, de Boer and co-workers<sup>1,2,4</sup> claim that the temperature dependence of spontaneous magnetization  $M(T,0)$  in the temperature interval  $0.1T_C \lesssim T \lesssim 0.75T_C$  ( $T_C$ = Curie point) is very well described by the expression  $M(T,0) = M(0,0) - aT^2$  yielded by the Stoner-Wohlfarth model,<sup>12,13</sup> which holds the Stoner single-particle spin-flip excitations solely responsible for the thermal demagnetization of  $M(T,0)$ . On the other hand, Sasakura, Suzuki, and Masuda<sup>10</sup> assert that  $M(T,0)$  follows the relations  $M^2(T,0) = M^2(0,0) - a'T^2$  and  $M^2(T,0) = a''(T_C^{4/3} - T^{4/3})$ , predicted by the spin-fluctuation (SF) model,<sup>14–21</sup> in the temperature ranges  $0.1T_C \lesssim T \lesssim 0.4T_C$  and  $0.42T_C \lesssim T \lesssim T_C$ , respectively. According to the SF model, nonpropagating thermally excited longitudinal and transverse spin-density fluctuations completely account for the decline of spontaneous magnetization with increasing temperature. In conflict with both the above-mentioned observations concerning the actual functional form of  $M(T,0)$ , small-angle neutron-scattering<sup>24</sup> (SANS) and inelastic neutron-scattering<sup>25</sup> (INS) experiments provide direct evidence for well-defined spin-wave excitations (i.e., for propagating thermally excited transverse spin-density fluctuations) in Ni<sub>3</sub>Al at temperatures in the range  $0.1T_C \lesssim T \lesssim 0.8T_C$ . Though the existence of spin waves at low temperatures in itinerant-

electron magnetic systems has been recognized<sup>26</sup> for a long time now, no indication for such excitations in Ni<sub>3</sub>Al has been found to date from magnetization measurements.

The spin-fluctuation (SF) theories (henceforth referred to as conventional SF theories) proposed hitherto are, to some extent, limited in scope in that they are unable to clarify the role of zero-point (quantum) spin fluctuations and fail to yield an expression which quantifies the suppression of local spin-density fluctuations by external magnetic field  $H_{ext}$ . Obviously, the theoretical limitations of this kind seriously hamper the understanding of magnetism in weak itinerant-electron (WI) ferromagnets such as Ni<sub>3</sub>Al. Recently, Kaul and co-workers<sup>27,28</sup> have addressed these deficiencies of the conventional SF theories from the theoretical point of view and remedied them by a self-consistent treatment of the SF model, which makes use of the Ginzburg-Landau formalism. Kaul and co-workers<sup>27,28</sup> have explicitly calculated the zero-point (ZP) and thermally excited (TE) contributions to spin fluctuations in WI ferromagnets in the presence and absence of  $H_{ext}$  and the results (briefly summarized in the next section; the details are given in Ref. 28) demonstrate the following. ZP spin fluctuations (i) have a major share in renormalizing the Landau coefficients of the Stoner-Wohlfarth theory, (ii) are relatively insensitive to  $H_{ext}$ , and (iii) make an appreciable contribution to the temperature dependence of magnetization. By contrast, TE collective electron-hole pair excitations almost entirely account for the dependences of magnetization on temperature and field, and get strongly suppressed by  $H_{ext}$ . In addition, this theoretical approach<sup>27,28</sup> for the first time, yields an analytical expression for the suppression of TE spin fluctuations by magnetic field for temperatures just outside the critical region but below the Curie point  $T_C$ .

Extensive high-resolution bulk magnetization measurements were undertaken on well-characterized Ni<sub>3</sub>Al sample with a view to resolve the controversy surrounding the nature of low-lying magnetic excitations and to test the validity of

the theoretical predictions mentioned above. An elaborate analysis of the magnetization  $M(T, H)$  data reveals that the thermal demagnetization of  $M(T, H)$  is primarily due to spin-wave excitations at low temperatures ( $0.09T_C \leq T \leq 0.28T_C$ ) and enhanced local spin-density fluctuations over a wide range of temperatures  $0.32T_C \leq T \leq 0.92T_C$ . Spin-wave stiffness  $D$  is independent of  $H_{ext}$  and possesses a value that is in excellent agreement with those determined previously<sup>24,25</sup> from SANS and INS measurements. In accordance with the theoretical predictions,<sup>27,28</sup> thermally excited spin fluctuations are found to be far more sensitive to magnetic field than zero-point spin fluctuations and the observed field dependence of  $M(T, H)$  in the temperature range  $0.5T_C \leq T \leq 0.92T_C$  is reproduced in facsimile by the analytical expression yielded by the theory. Moreover, the present work permits an unambiguous assessment of the relative importance of thermally excited and zero-point components of spin fluctuations in a weak itinerant-electron ferromagnet.

## II. THEORETICAL CONSIDERATIONS

In this section, a brief outline of the *self-consistent* calculation<sup>28</sup> of spin fluctuations in weak itinerant-electron ferromagnets based on the version of spin-fluctuation theory that makes use of the Ginzburg-Landau (GL) formalism is given. The results of this calculation put most of our observations on a consistent theoretical footing, as will be shown to be the case in a later section.

The thermal variances of the local magnetization (a small slowly varying *classical* order parameter) parallel ( $\parallel$ ),  $\langle m_{\parallel}^2 \rangle$ , and perpendicular ( $\perp$ ),  $\langle m_{\perp}^2 \rangle$ , to the average magnetization  $\vec{M}$  are related to the imaginary part of the dynamic wave-vector-dependent susceptibility,  $\text{Im}\chi_{\nu}(\vec{q}, \omega)$ , where  $\nu(\parallel, \perp)$  is the polarization index, through the well-known fluctuation-dissipation relation<sup>17–22,27,28</sup>

$$\langle m_{\nu}^2 \rangle = 4\hbar \int \frac{d^3\vec{q}}{(2\pi)^3} \int \frac{d\omega}{2\pi} \left( n(\omega) + \frac{1}{2} \right) \text{Im}\chi_{\nu}(\vec{q}, \omega) \quad (1)$$

with

$$n(\omega) = [\exp(\hbar\omega/k_B T) - 1]^{-1}, \quad (2)$$

$$\text{Im}\chi_{\nu}(\vec{q}, \omega) = \omega\chi_{\nu}(\vec{q}) \frac{\Gamma_{\nu}(\vec{q})}{\omega^2 + \Gamma_{\nu}^2(\vec{q})}, \quad (3)$$

$$\chi_{\nu}(\vec{q}) = \chi_{\nu}(\vec{q}, \omega=0) = \chi_{\nu}(0) \frac{\kappa_{\nu}^2}{\kappa_{\nu}^2 + q^2}, \quad (4)$$

$$\Gamma_{\nu}(\vec{q}) = \gamma_{\nu} q \chi_{\nu}^{-1}(\vec{q}) = \Gamma_{\nu}(0) q (\kappa_{\nu}^2 + q^2), \quad (5)$$

$$\chi_{\nu}(0) = \chi_{\nu}(\vec{q}=0) = (c_{\nu} \kappa_{\nu}^2)^{-1}, \quad (6)$$

$$\Gamma_{\nu}(0) = \Gamma_{\nu}(\vec{q}=0) = c_{\nu} \gamma_{\nu}, \quad (7)$$

where  $n(\omega)$  is the Bose function,  $\Gamma_{\nu}(\vec{q})$  is the relaxation frequency of a spontaneous spin fluctuation of wave vector  $\vec{q}$  and polarization  $\nu$ ,  $\chi_{\nu}(0)$  is the field- and temperature-dependent susceptibility [i.e.,  $\chi_{\nu}(0) \equiv \chi_{\nu}(T, H)$ ],  $c_{\nu}$  is the

coefficient of the gradient term in the GL expansion, and the quantity  $\gamma_{\nu}$  depends<sup>18</sup> on the shape of the density-of-states (DOS) curve near Fermi level  $E_F$ . According to Eq. (1), spin fluctuations are made up of two components, the zero-point spin fluctuations  $\langle m_{\nu}^2 \rangle^{ZP}$ , and the thermally excited (TE) spin fluctuations  $\langle m_{\nu}^2 \rangle^{TE}$ , represented in Eq. (1) by the factors  $1/2$  and  $n(\omega)$ , respectively. Zero-point spin fluctuations can be further split into two parts: quantum fluctuations at  $T=0$  K,  $\langle m_{\nu}^2 \rangle_0^{ZP}$ , and the temperature induced changes in quantum spin fluctuations at finite temperatures  $T \neq 0$ ,  $\langle m_{\nu}^2 \rangle_T^{ZP}$  (the so-called quantum dynamics). Thermally excited spin fluctuations too are of two types: damped (nonpropagating) longitudinal ( $\parallel$ ) and transverse ( $\perp$ ) spin fluctuations (SF) and undamped (propagating) transverse spin fluctuations or spin waves (SW).

So far as the ZP spin fluctuations are concerned, Eqs. (1)–(7) yield the final result<sup>28</sup>

$$\langle m_{\nu}^2 \rangle^{ZP} \simeq \frac{\hbar \gamma_{\nu}}{2(2\pi)^3} [q_C^{ZP}(T, H)]^2 \left( [q_C^{ZP}(T, H)]^2 [a_{\nu}^2 \ln(1 + a_{\nu}^{-2}) + \ln(1 + a_{\nu}^2)] - \frac{4}{c_{\nu} \chi_{\nu}(0)} [a_{\nu} \tan^{-1}(a_{\nu}^{-1})] \right) \quad (8)$$

with

$$a_{\nu} = \frac{v_F}{c_{\nu} \gamma_{\nu} [q_C^{ZP}(T, H)]^2}, \quad (9)$$

where  $v_F$  is the Fermi velocity and  $q_C^{ZP} \equiv q_C^{ZP}(T, H) = q_0(0, H) + q_C(T, H)$  is the temperature- and field-dependent cutoff wave vector.  $q_C^{ZP}$  approaches a very small but finite value  $q_0$  as  $T \rightarrow 0$  K. The above expression, Eq. (8), for  $\langle m_{\nu}^2 \rangle^{ZP}$  is valid in the entire temperature range extending from  $T=0$  K to temperatures well above  $T_C$ . By contrast, a similar expression for the thermally excited component of spin fluctuations  $\langle m_{\nu}^2 \rangle^{TE}$ , that holds for temperatures in the range  $0 \leq T \leq T_C$ , cannot be obtained from Eqs. (1)–(7) since Eq. (1) is not amenable to analytical solution primarily because different types of TE spin fluctuations dominate in different temperature ranges.

At low temperatures, the main contribution to  $\langle m_{\nu}^2 \rangle^{TE}$  arises from long-wavelength ( $q \lesssim q_{SW}$ ) low-frequency spin waves. Such a contribution is obtained from Eq. (1) by inserting the following expression<sup>18</sup> for  $\text{Im}\chi_{\nu}(\vec{q}, \omega)$  in this equation, and then evaluating the integrals:

$$\text{Im}\chi_{\nu}(\vec{q}, \omega) = \frac{\pi}{2} \omega \chi_{\perp}(\vec{q}) [\delta(\omega - \omega(\vec{q})) + \delta(\omega + \omega(\vec{q}))] \quad (10)$$

with the spin wave propagation frequency  $\omega(\vec{q})$  given by<sup>18</sup>

$$\hbar \omega(\vec{q}) = g \mu_B H + D_{\perp}^{SW}(T, H) q^2 + \dots, \quad (11)$$

where the effective field  $H$  is the external magnetic field  $H_{ext}$ , corrected for demagnetizing field  $H_{dem}$  and other anisotropy fields  $H_A$ , i.e.,  $H = H_{ext} - H_{dem} + H_A = H_{ext} - 4\pi N M(T, H_{ext}) + H_A$ ,  $N$  is the demagnetizing factor,  $g$  is

the Landé splitting factor, and  $D_{\perp}^{SW}(T, H) = g \mu_B M(T, H) c_{\perp}$  is the spin-wave stiffness. Equation (1), when combined with Eqs. (10) and (11), gives ultimately the spin-wave contribution as

$$\begin{aligned} \langle m_{\perp}^2 \rangle_{SW}^{TE} &= \zeta(3/2) g \mu_B M(T, 0) \left[ \frac{k_B T}{4 \pi D_{\perp}^{SW}(T, 0)} \right]^{3/2} \\ &\text{for } H=0, \\ &= Z(3/2, t_H) g \mu_B M(T, H) \left[ \frac{k_B T}{4 \pi D_{\perp}^{SW}(T, H)} \right]^{3/2} \\ &\text{for } H \neq 0. \end{aligned} \quad (12)$$

In Eq. (12), the Bose-Einstein integral function  $Z(3/2, t_H) = \zeta(3/2) F(3/2, t_H) = \sum_{n=1}^{\infty} n^{-3/2} e^{-nt_H}$  with  $t_H = g \mu_B H / k_B T$  allows for the energy gap in the spin-wave spectrum introduced by  $H_{ext}$  and the anisotropy fields.

In the intermediate range of temperatures and for temperatures close to  $T_C$ , spin-wave contribution is completely masked by the one arising from nonpropagating spin fluctuations (SF). In this temperature range, Eqs. (1)–(7) can be solved for the contribution due to TE spin fluctuations, i.e.,  $\langle m_{\nu}^2 \rangle_{SF}^{TE}$ , by using the so-called classical approximation. This approximation implies that each mode  $m_{\nu}(\vec{q})$  for  $\vec{q} < \vec{q}_c$  is thermally excited such that the Bose function, Eq. (2), can be approximated by  $k_B T / \hbar \omega$  for those values of  $\omega$  for which  $\text{Im} \chi_{\nu}(\vec{q}, \omega)$  makes appreciable contribution to the integral over  $\omega$  in Eq. (1). Such an approximation leads to the result

$$\langle m_{\nu}^2 \rangle_{SF}^{TE} = \frac{k_B T}{2 \pi^2 c_{\nu}} [q_c^{TE} - \kappa_{\nu} \tan^{-1}(q_c^{TE} / \kappa_{\nu})] \quad (13)$$

with  $q_c^{TE} \equiv q_c \equiv q_c(T, H)$ . Equation (13) reduces to<sup>28</sup>

$$\langle m_{\nu}^2 \rangle_{SF}^{TE} = \left( \frac{k_B T}{6 \pi^2} \right) \chi_{\nu}(0) q_c^3 \quad (14)$$

and

$$\begin{aligned} \langle m_{\nu}^2 \rangle_{SF}^{TE} &= \left( \frac{k_B T}{2 \pi^2} \right) \left( \frac{q_c}{c_{\nu}} \right) \left[ 1 - \frac{\pi}{2 q_c} \left( \frac{g \mu_B}{D_{\nu}^{SF}} \right)^{1/2} H^{1/2} \right. \\ &\quad \left. + \frac{1}{q_c^2} \left( \frac{g \mu_B}{D_{\nu}^{SF}} \right) H \right] \end{aligned} \quad (15)$$

at intermediate temperatures and for temperatures close to  $T_C$  ( $T \lesssim T_C$ ) but outside the critical region, respectively. In Eq. (15),  $D_{\nu}^{SF} = g \mu_B M(T, H) c_{\nu}$  is the so-called spin-fluctuation stiffness. The temperature- and field-dependent cutoff wave vector  $q_c$  appearing in Eqs. (8), (9), (14), and (15) is given by<sup>27,28</sup>

$$q_c(T, H) = \left( \frac{k_B T}{\hbar c_{\nu} \gamma_{\nu}} \right)^{1/3} \left( 1 - x + \frac{x^3}{3} \right) \quad (16)$$

with

$$x = \frac{1}{3 c_{\nu} \chi_{\nu}(0)} \left( \frac{\hbar \gamma_{\nu} c_{\nu}}{k_B T} \right)^{2/3}. \quad (17)$$

The variations of magnetization with temperature and field are obtained in a self-consistent fashion by inserting the expressions for  $\langle m_{\nu}^2 \rangle = \langle m_{\nu}^2 \rangle^{ZF} + \langle m_{\nu}^2 \rangle^{TE}$  valid in different temperature ranges into the following expression,<sup>18</sup> which is nothing but the Stoner magnetic equation of state (MES) modified to account for long-wavelength and low-energy spin fluctuations of small fluctuation amplitudes, i.e., in

$$\frac{H}{M(T, H)} = a(T) + b[(3 \langle m_{\parallel}^2 \rangle + 2 \langle m_{\perp}^2 \rangle) + M^2(T, H)] \quad (18)$$

with

$$a(T) = -[2 \chi(0, 0)]^{-1} \left[ 1 - \left( \frac{T}{T_C^S} \right)^2 \right], \quad (19)$$

$$b = [2 \chi(0, 0) M^2(0, 0)]^{-1}, \quad (20)$$

where  $\chi(0, 0)$  is the zero-field differential susceptibility at 0 K and  $T_C^S$  is the Stoner Curie temperature. The final outcome of this exercise is that the coefficients  $a(T)$  and  $b$  of the Stoner MES get renormalized<sup>28</sup> and  $M(T, H)$  takes the forms

$$\begin{aligned} M(T, 0) &= M(0, 0) - g \mu_B \zeta(3/2) [k_B T / 4 \pi D_{\perp}^{SW}(T, 0)]^{3/2}, \\ &H=0 \end{aligned} \quad (21a)$$

$$\begin{aligned} M(T, H) &= M(0, H) - g \mu_B Z(3/2, t_H) [k_B T / 4 \pi D_{\perp}^{SW}(T, H)]^{3/2}, \\ &H \neq 0 \end{aligned} \quad (21b)$$

at low temperatures,

$$M(T, H) = M(0, H) [1 - (T/T^*)^2 - (T/T_1)^{4/3}]^{1/2}, \quad (22)$$

where

$$\left( \frac{1}{T^*} \right)^2 = \left( \frac{1}{T_C^S} \right)^2 + \left( \frac{1}{T_0} \right)^2, \quad (23)$$

$$T_0^{-2} = \frac{1}{6 \pi^2} \left( \frac{k_B^2}{\hbar \gamma_{\nu} c_{\nu}} \right) \left( \frac{3 \chi_{\parallel}(0) + 2 \chi_{\perp}(0)}{M^2(0, 0)} \right), \quad (24)$$

$$\begin{aligned} T_1^{-4/3} &\equiv \frac{5}{2 \pi^2} \left( \frac{3 + 6 \ln a_{\nu} - 8 \pi}{24 \pi} \right) \\ &\quad \times (\hbar \gamma_{\nu})^{-1/3} [M(0, 0)]^{-2} \left( \frac{k_B}{c_{\nu}} \right)^{4/3} \end{aligned} \quad (25)$$

at intermediate temperatures, and

$$M(T, H) = M(0, H) [1 - (T/T_C^S)^2 - A(H) T^{4/3}]^{1/2}, \quad (26)$$

with

$$A(H) = A(H=0) [1 - \eta \sqrt{H}], \quad (27)$$

$$A(H=0) = (T_C^{SF})^{-4/3} \cong \frac{5(1+2 \ln a_\nu + 8\pi)}{16\pi^3} (\hbar \gamma_\nu)^{-1/3} \\ \times [M(0,0)]^{-2} \left( \frac{k_B}{c_\nu} \right)^{4/3}, \quad (28)$$

$$\eta \cong \frac{4\pi^2}{1+2 \ln a_\nu + 8\pi} \left( \frac{k_B T}{\hbar \gamma_\nu c_\nu} \right)^{-1/3} \left( \frac{g\mu_B}{D_\nu^{SF}} \right)^{1/2} \quad (29)$$

for temperatures close to  $T_C$  ( $T \lesssim T_C$ ) but outside the critical region. Equations (22) and (26) are valid for both  $H=0$  and  $H \neq 0$ . While the  $T^2$  term (with the coefficient  $T_0^{-2}$ ) in Eq. (22) originates from thermally excited nonpropagating spin fluctuations and its coefficient  $T_0^{-2}$  depends on  $H$  through the field dependence of  $\chi_\nu(0)$ , the  $T^{4/3}$  term is a net outcome of the competing claims made by the thermally excited (TE) and zero-point (ZP) components of spin fluctuations (the former contribution decreases with  $T$  as  $T^{4/3}$  whereas the latter one dominates over the former and increases with  $T$  as  $T^{4/3}$ ) and its coefficient  $T_1^{-4/3}$  is essentially field independent. Due to the competition between ZP and TE components, the  $T^2$  term accounts, in the most part, for  $M(T,H)$  but the contribution of the  $T^{4/3}$  term is not so small as to warrant its total neglect. By contrast, the  $T^{4/3}$  term in Eq. (26) is a direct consequence of the additive TE and ZP spin-fluctuation contributions, both of which increase with  $T$  as  $T^{4/3}$  for  $T \lesssim T_C$ , but the TE contribution now dominates over the ZP one. Moreover, the coefficient  $A(H)$  of this term depends on the field in accordance with the relation (27) and the field dependence of  $A$  is entirely due to the suppression of TE spin fluctuations by  $H$ .

The calculations, briefly outlined above and whose details are given in Ref. 28, go beyond the conventional SF theories in that they (i) bring out clearly the role of zero-point spin fluctuations in affecting the functional dependences of magnetization on temperature and field, (ii) predict an additional contribution to  $M(T,H)$  at intermediate temperatures which varies with  $T$  as  $T^{4/3}$  but does not depend on the field  $H$ , (iii) demonstrate that at all temperatures, field suppresses thermally excited spin fluctuations but has little, or even no, effect on zero-point spin fluctuations, and (iv) quantify the suppression of TE spin fluctuations with magnetic field in the form of Eqs. (26), (27), and (29) for  $T \lesssim T_C$ .

### III. EXPERIMENTAL DETAILS

Ultra-high-purity (99.999) nickel and aluminum taken in stoichiometric proportions by weight were molten together in a recrystallized alumina crucible under an inert atmosphere provided by high-purity (99.999) argon gas by radio frequency induction technique. After holding the melt for a couple of minutes in the crucible, it was poured into a cylindrical hole in a massive copper mold. The entire operation from melting to pouring was carried out under argon pressure of  $>1$  atm. Polycrystalline  $\text{Ni}_3\text{Al}$  was thus prepared in the rod (10 mm in diameter and 100 mm in length) form. Several discs of 5 mm thickness were spark cut from such a rod and characterized by x-ray-diffraction and scanning electron microscopic techniques. The chemical composition of samples taken from various sections along the rod length was

determined by methods such as x-ray fluorescence, inductively coupled plasma, and optical emission spectroscopy. Ni (Al) composition in at. % varied in the range 74.7 (25.3) to 75.0 (25.0) over the entire length of the rod. The portion of the  $\text{Ni}_3\text{Al}$  rod whose composition did not deviate more than 0.01 at. % from the stoichiometric composition  $\text{Ni}_{75}\text{Al}_{25}$  was selected, spherical (3 mm in diameter) and disc shaped (10 mm in diameter and 5 mm in thickness) samples were spark cut from it and annealed at  $520^\circ\text{C}$  for 16 days in quartz tubes evacuated to a pressure of  $10^{-7}$  torr. Spherical and disc-shaped samples were used for magnetic and x-ray-diffraction measurements, respectively. The observed x-ray patterns could be completely indexed on the basis of the  $L1_2$  cubic structure with lattice constant  $a=3.564(2)$  Å. This lattice parameter value is in excellent agreement with that [ $a=3.565(5)$  Å] reported<sup>29,30</sup> in the literature. From the observed integrated intensities  $I_F$  and  $I_S$  of the (200) fundamental ( $F$ ) fcc-type and (100) superstructure ( $S$ )  $\text{Cu}_3\text{Au}$ -type Bragg reflection peaks, long-range order parameter  $S$  was estimated using the relation  $S^2 = (I_S/I_F)_{\text{sample}} \times (I_F/I_S)_{S=1}$ , where  $(I_F/I_S)_{S=1}$  is the corresponding intensity ratio<sup>29</sup> for fully ordered  $\text{Ni}_3\text{Al}$  sample. For the  $\text{Ni}_3\text{Al}$  sample used for the present investigation, we obtain  $S=0.55(1)$ .

Magnetization  $M$  of the  $\text{Ni}_3\text{Al}$  sample (spherical in shape) was measured as a function of external magnetic field  $H_{\text{ext}}$  in fields up to 15 kOe (70 kOe) at fixed temperatures (at  $T=5$  K),  $\approx 0.5, 0.2, 0.1,$  and  $0.05$  K apart in the ranges  $14.7 \leq T \leq 40.4$  K,  $40.4 \leq T \leq 50$  K,  $50 \leq T \leq 51.5$  K, and  $51.5 \leq T \leq 58.5$  K, respectively, on EG&G Princeton Applied Research Vibrating Sample Magnetometer (VSM) 4500 system [Quantum Design superconducting quantum interference device (SQUID) magnetometer MPMS7]. Each  $M-H_{\text{ext}}$  isotherm (the isotherm at 5 K) was obtained by measuring  $M$  at 60 (180) predetermined fixed field values in the range  $0 \leq H_{\text{ext}} \leq 15$  kOe ( $0 \leq H_{\text{ext}} \leq 70$  kOe). Magnetization was also measured as a function of temperature in the interval  $14 \leq T \leq 80$  K ( $5 \leq T \leq 100$  K) at fixed values of  $H_{\text{ext}}$  (at  $H_{\text{ext}}=1$  kOe), 0.5 kOe apart, in the interval  $0.5 \leq H_{\text{ext}} \leq 4$  kOe on VSM (SQUID). The ‘‘in-field’’ magnetization, i.e.,  $M(T)$  at fixed  $H_{\text{ext}}$  and denoted by  $M(T, H_{\text{ext}})$ , data were taken at the temperature steps of 0.25 and 0.5 K in the temperature ranges  $14 \leq T \leq 50.5$  K and  $50.5 \leq T \leq 80$  K, respectively. The temperature (field) stability was better than  $\pm 5$  mK ( $\pm 10$  Oe) for the VSM data and  $\pm 10$  mK ( $\pm 1$  Oe) for the SQUID data. In the present case, magnetization was measured to a relative accuracy of 50 ppm (1 ppm) using VSM (SQUID) magnetometer. The  $M$  versus  $H_{\text{ext}}$  isotherms were converted into a form that gives the magnetization as a function of temperature at 60 different but fixed values of  $H_{\text{ext}}$  in the interval  $0.3 \leq H_{\text{ext}} \leq 15$  kOe. Such data are henceforth referred to as the ‘‘in-field’’ (iso) magnetization data and labeled as  $M'(T, H_{\text{ext}})$ . The demagnetizing factor  $N$  was computed from the slope of the magnetization versus  $H_{\text{ext}}$  straight line [i.e.,  $4\pi N = (\text{slope})^{-1}$ ] isotherms taken at temperatures well below  $T_C$  in the field range  $-20 \leq H_{\text{ext}} \leq 20$  Oe. The value  $N$ , so obtained, was used to arrive at the effective field  $H$  experienced by the spins in the  $\text{Ni}_3\text{Al}$  sample, i.e.,  $H = H_{\text{ext}} - 4\pi N M(T, H_{\text{ext}})$ .

### IV. DATA ANALYSIS, RESULTS, AND DISCUSSION

$[M(T,H)]^2$  versus  $H/M(T,H)$  (Arrott) plots at different temperatures, based on the magnetic equation of state, Eq.

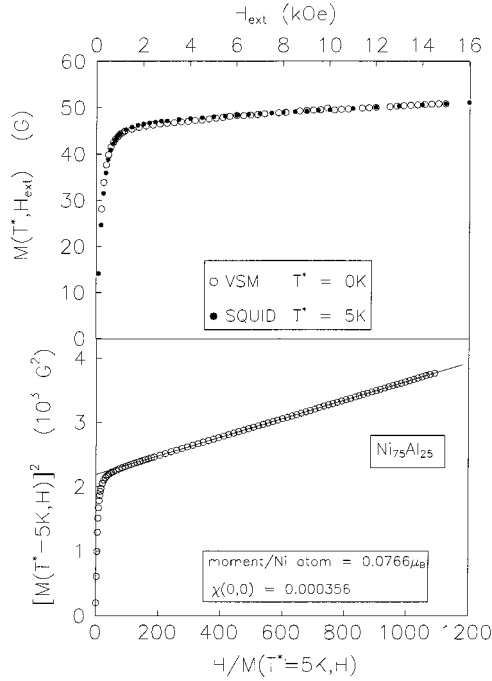


FIG. 1. The upper part of the figure compares the  $M$  versus  $H_{ext}$  isotherm taken at 5 K (the SQUID data) with the values of  $M$  at  $T=0$  deduced from the fits, based on Eq. (21b) of the text, to the  $M(T)$  data taken at different values of  $H_{ext}$ . The lower part shows the magnetization at  $T=5$  K measured in fields ( $H_{ext}$ ) up to 70 kOe plotted in the form of the Arrott plot, i.e.,  $[M(T=5 \text{ K}, H)]^2$  versus  $H/M(T=5 \text{ K}, H)$  plot.

(18), and constructed out of the raw  $M(T, H_{ext})$  data, are displayed in the bottom panel of Fig. 1 (SQUID data at  $T=5$  K) and Fig. 2 (VSM data at  $T \geq 14.7$  K). Spontaneous magnetization at different temperatures  $M(T, 0)$  is computed

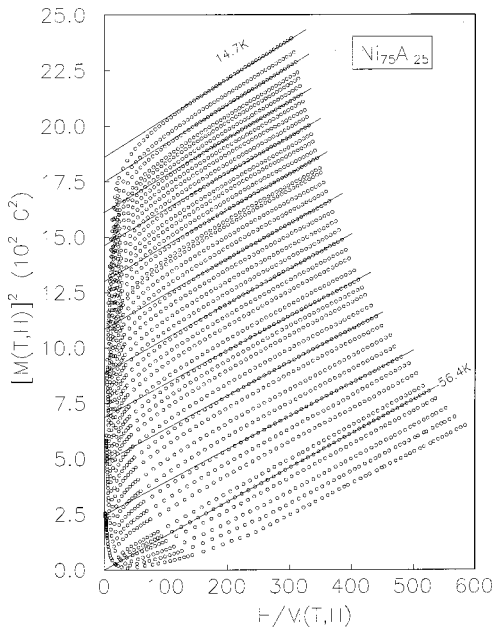


FIG. 2.  $[M(T, H)]^2$  versus  $H/V(T, H)$  isotherms at a few representative temperatures. Note that the linear isotherm at  $T=T_C=56.4$  K passes through the origin.

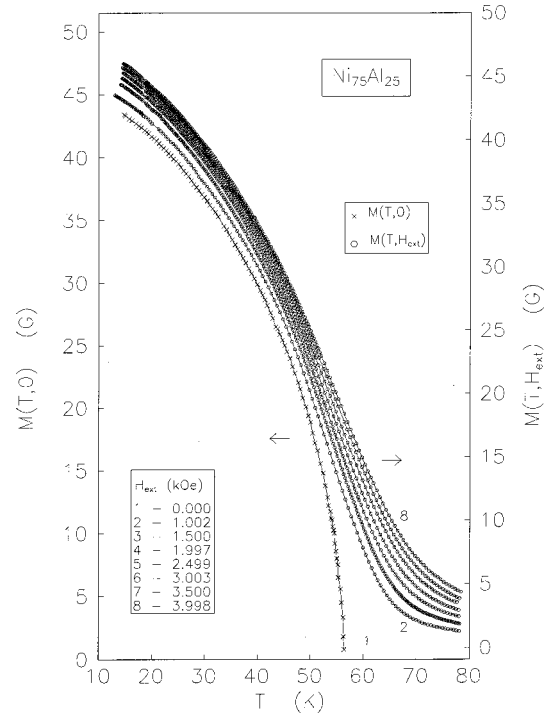


FIG. 3. Spontaneous magnetization  $M(T, 0)$  and in-field magnetization  $M(T, H_{ext})$ , as functions of temperature.

from the intercepts on the ordinate obtained by extrapolating the linear high-field portions of the Arrott plot isotherms to  $H=0$ , as shown in Figs. 1 and 2. The  $M(T, 0)$  data, so obtained, together with the in-field magnetization data at a few selected values of  $H_{ext}$  in the interval  $1 \leq H_{ext} \leq 4$  kOe, are depicted in Fig. 3. The  $M-H_{ext}$  isotherm at  $T=5$  K measured on SQUID magnetometer in fields up to 70 kOe, when converted into the Arrott isotherm shown in the bottom panel of Fig. 1, yields the values  $M(T=5 \text{ K}, 0) = 46.75(12)$  G or  $0.0766(2) \mu_B/\text{Ni atom}$  and  $\chi(T=5 \text{ K}, 0) = 3.56(30) \times 10^{-4}$  for the spontaneous magnetization or magnetic moment per nickel atom and zero-field differential susceptibility at 5 K. These magnitudes are in excellent agreement with those reported<sup>1,2,10,11</sup> previously. From the Arrott plot shown in Fig. 2, we obtain the Curie temperature for the present sample as  $T_C = 56.45(5)$  K [i.e., the temperature at which the linear  $M^2$  vs  $H/M$  isotherm passes through the origin or alternatively, the temperature at which  $M(T, 0)$  goes to zero, Fig. 3]. This value agrees quite well with that obtained by the ‘‘kink-point’’ method but is substantially higher than the published<sup>1,2,10,11</sup> values.

In view of the conflicting reports<sup>1,2,4,10</sup> about the temperature dependence of  $M(T, 0)$  at low and intermediate temperatures in Ni<sub>3</sub>Al (see Introduction), the magnetization data are analyzed in terms of the expressions predicted by the Stoner-Wohlfarth (SWO) model,<sup>12,13</sup> conventional spin fluctuation (CSF) theories<sup>14–21</sup> and the modified spin fluctuation (MSF) model<sup>27,28</sup> briefly outlined in Sec. II. Before embarking upon such an analysis, the relevant expressions for magnetization yielded by such theories are given below. According to the SWO model, magnetization for both  $H=0$  and  $H \neq 0$  in the entire temperature range  $0 \leq T \leq T_C$  is given by<sup>2,12,13,31</sup>

$$[M(T, H)]_{SWO} = M(0, H)[1 - a(H)T^2]$$

with

$$a(H=0) = (T_C^S)^{-2}. \quad (30)$$

By contrast, CSF and MSF theories predict different expressions for magnetization in different temperature regions. For instance, magnetization is described, by Eqs. (21a) and (21b) at low temperatures, by the expressions<sup>18,28</sup>

$$[M(T,H)]_{CSF} = M(0,H)[1 - a'(H)T^2]^{1/2}, \quad (31)$$

$$[M(T,H)]_{MSF} = M(0,H)[1 - A'(H)T^2 - A''T^{4/3}]^{1/2} \quad (32)$$

[cf. Eq. (32) with Eqs. (22)–(25)] at intermediate temperatures and by

$$[M(T,H)]_{CSF} = M(0,H)[1 - a''(H)T^{4/3}]^{1/2} \quad (33)$$

$$[M(T,H)]_{MSF} = M(0,H)[1 - A(H)T^{4/3}]^{1/2} \quad (34)$$

[cf. Eq. (34) with Eqs. (26)–(29)] for temperatures close to  $T_C$  ( $T \lesssim T_C$ ) and yet away from criticality. Note that Eqs. (32) and (34) are valid for both  $H \neq 0$  and  $H = 0$  whereas Eqs. (31) and (33) hold for  $H = 0$  only. Moreover, the coefficients of the  $T^{4/3}$  terms in Eqs. (33) and (34) for  $H = 0$  are completely different; i.e.,  $a''(0) \neq A(H = 0)$ .

The  $M(T,H)$ ,  $M'(T,H)$  and  $M(T,0)$  data have been analyzed in terms of Eqs. (21a), (21b) and (30)–(34) using the ‘‘range-of-fit’’ (ROF) analysis. In this type of analysis, the values of free fitting parameters and the quality of the fits are continuously monitored as the temperature interval  $T_{min} \leq T \leq T_{max}$  is progressively narrowed down by keeping  $T_{min}(T_{max})$  fixed at a given value and lowering (raising)  $T_{max}(T_{min})$  towards  $T_{min}(T_{max})$ . The details about this method of analysis are given elsewhere.<sup>31–33</sup> In the absence of the spontaneous and ‘‘in-field’’ (VSM) magnetization data for  $T < 14$  K, the ROF analysis of the  $M(T,H)$  SQUID data taken at  $H_{ext} = 1$  kOe (that extend down to 5 K) in the low-temperature region has been attempted based on Eqs. (30), (21b), and (31). In this analysis,  $M(0,H)$  and  $a(H)$  in Eq. (30),  $M(0,H)$  and spin-wave stiffness  $D \equiv D_{\perp}^{SW}$  in Eq. (21b), and  $M(0,H)$  and  $a'(H)$  in Eq. (31) are treated as free fitting parameters. The final outcome of this exercise is that Eq. (21b) reproduces in facsimile the observed temperature dependence of magnetization in the temperature interval  $5 \leq T \leq 13$  K. The best least-squares (LS) fit to the data (open circles) in this temperature range, based on Eq. (21b), yields  $D = 69.6$  meV  $\text{\AA}^2$  and is depicted in the upper part of Fig. 4 by the continuous curve. The lower part of Fig. 4 shows the percentage deviation of the data from the best LS fits based on Eq. (30) (open circles), Eq. (21b) (solid circles) and Eq. (31) (crosses) in the temperature interval  $5 \leq T \leq 13$  K. It is evident from this figure that the percentage deviation of the  $M(T,H)$  data from the best  $M - T^{3/2}$  fit, based on Eq. (21b), does not exceed  $\pm 0.003$  and is evenly distributed around the theoretically calculated values whereas the optimum  $M - T^2$  and  $M^2 - T^2$  fits, based on Eqs. (30) and (31), respectively, present systematic deviations from the data in question that are, in both the cases, as large as  $\pm 0.08\%$ . Another important observation is that if  $T_{min}$  is fixed at 5 K and  $T_{max}$  is increased beyond 13 K, the deviations of the data from the

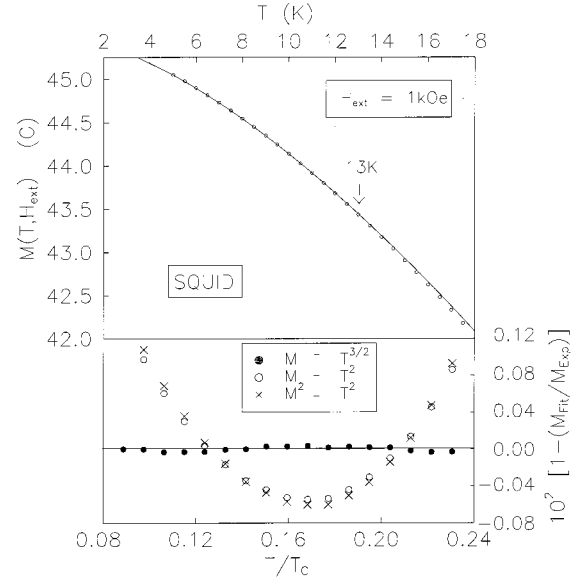


FIG. 4. The upper part of the figure depicts temperature variation of magnetization measured at  $H_{ext} = 1$  kOe at low temperatures and the continuous curve through the data points (open circles) is the best least-squares (LS) fit based on Eq. (21b) of the text. The lower part displays the percentage deviation of the data from the LS fits based on Eq. (21b) (closed circles), Eq. (30) (open circles), and Eq. (31) (crosses), of the text.

$M - T^{3/2}$  fit continue to remain evenly distributed but increase steadily to reach  $\pm 0.005\%$  at  $T_{max} = 16$  K with marginal change in the values of fitting parameters  $M(0,H)$  and  $D$  whereas they are systematic in nature and grow very fast for  $T_{max} > 16$  K and lead to a steep fall (increase) in the value of  $D$  ( $M(0,H)$ ). The latter observation encouraged us to attempt  $M - T^{3/2}$  fits to ‘‘in-field’’ ( $0.5 \leq H_{ext} \leq 4.0$  kOe) and in-field (iso) ( $0.5 \leq H_{ext} \leq 15$  kOe) magnetization data as well as to the  $M(T,0)$  data based on Eqs. (21b) and (21a) in the temperature range ( $14 \leq T \leq 16$  K). The range-of-fit analysis of the  $M(T,0)$  and  $M(T,H)$  data in which  $M(0,0)$  or  $M(0,H)$  or  $M'(0,H)$  and  $D$  are varied to optimize agreement between theory and experiment revealed that (i) Eqs. (21a) and (21b) provide the best description of the data for  $T \leq 16$  K  $\approx 0.28T_C$  [continuous curves in the inset of Fig. 5(b)], (ii) spin-wave stiffness possesses the value  $D = 69.6(4)$  meV  $\text{\AA}^2$  regardless of the magnitude of field in the interval  $0 \leq H_{ext} \leq 15$  kOe, and (iii) the  $M(0,H_{ext})$  values yielded by the best LS fits conform very well (upper part of Fig. 1) with the  $M(T,H_{ext})$  values measured on SQUID magnetometer at  $T = 5$  K. Moreover, the modified versions of Eqs. (21a) and (21b), that take into account the temperature renormalization of  $D$ , when used for the analysis, did not bring forth any improvement in the quality of fits. Considering the variation in the value of  $D$  not only for a given data set but also from one set to the other as the temperature range of the fit is changed, we quote the final value  $D = 69.6(14)$  meV  $\text{\AA}^2$  in the temperature interval  $0.09T_C \leq T \leq 0.28T_C$  with conservative assignment of errors. This value compares favorably with  $D = 70(20)$  meV  $\text{\AA}^2$  [ $D = 85(15)$  meV  $\text{\AA}^2$ ] determined in the temperature range  $5 \leq T \leq 15$  K (at  $T = 20.4$  K) from small-angle neutron-scattering<sup>24</sup> (inelastic neutron-scattering<sup>25</sup>) data. From a de-

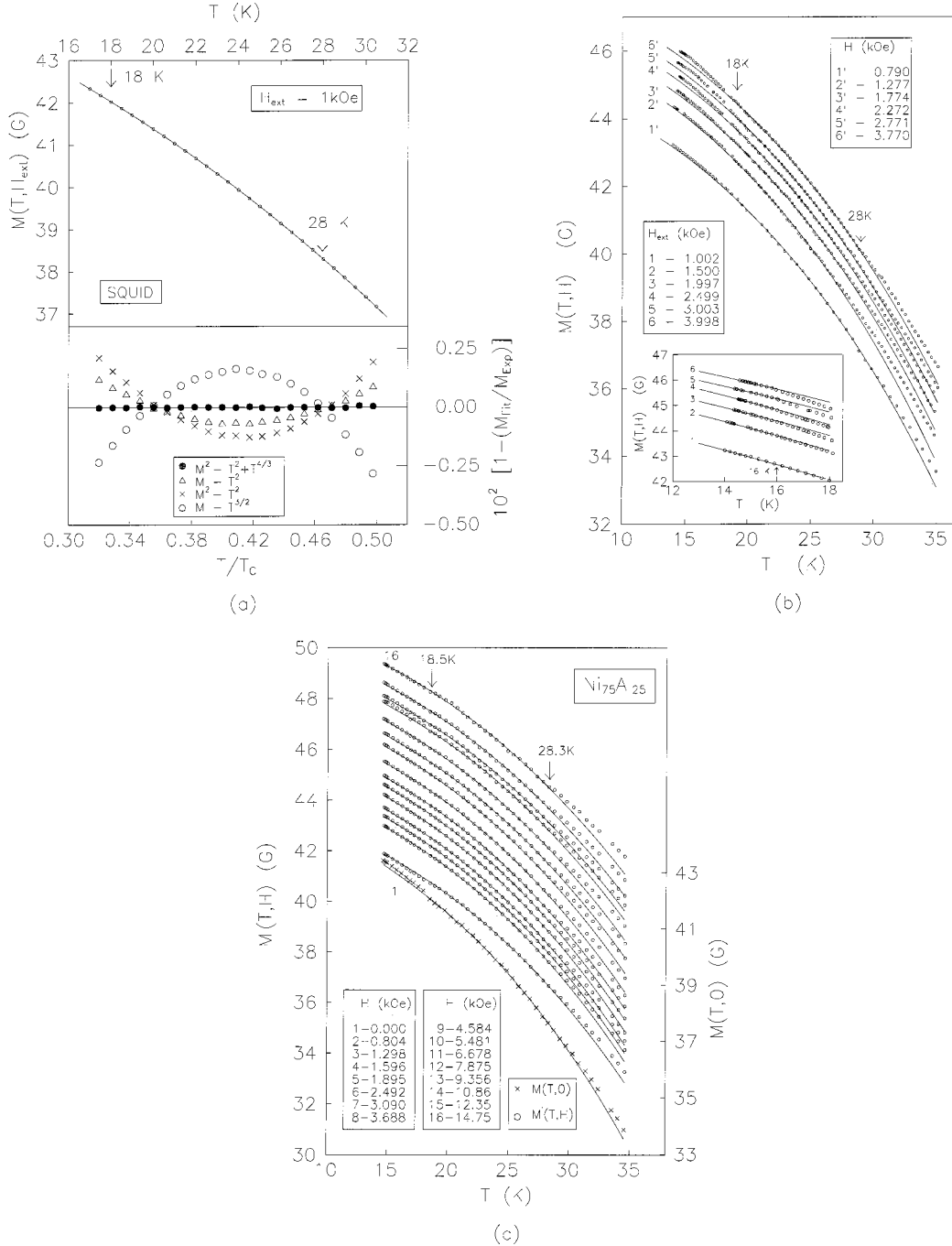


FIG. 5. Temperature variation of in-field magnetization, (a)  $M(T, H_{ext} = 1 \text{ kOe})$ , (b)  $M(T, H)$ , and (c)  $M'(T, H)$ , at a few selected but fixed values of  $H$  in the intermediate range of temperatures. Part (c) of the figure, in addition, depicts the temperature dependence of spontaneous magnetization  $M(T, 0)$  in this temperature range. The continuous curves through the  $M(T, H)$  data (open circles) and  $M(T, 0)$  data (crosses) represent the best least-squares fits based on Eq. (32) of the text. Lower panel of Fig. 5(a) displays the percentage deviation of the  $M(T, H_{ext} = 1 \text{ kOe})$  SQUID data from the fits based on Eq. (21b) (open circles), Eq. (30) (open triangles), Eq. (31) (crosses), and Eq. (32) (closed circles), of the text. Inset of Fig. 5(b) shows the least-squares fits (continuous curves) based on Eq. (21b) to the  $M(T, H)$  data taken at various fixed values of  $H$ .

tailed comparison between the different types of theoretical fits to the magnetization data (Fig. 4) and the agreement between the values of spin-wave stiffness determined by different experimental techniques, we conclude that spin-wave excitations dominantly contribute to the thermal demagnetization of both spontaneous as well as in-field magnetization for temperatures  $T \leq 0.28T_c$ .

An exhaustive range-of-fit analysis of the  $M(T, H)$ ,

$M'(T, H)$ , and  $M(T, 0)$  data at intermediate temperatures and for  $T \leq T_c$  based on Eqs. (21a) and (30)–(34) yields a number of important results. In the intermediate range of temperatures, the main observations are as follows. (I) Out of all the theoretical expressions considered, Eq. (32) alone provides the best LS fit (depicted by the continuous curves in Fig. 5) to the magnetization data at all fields including  $H = 0$  in the temperature range  $18 \text{ K} (\approx 0.32T_c) \leq T \leq 28 \text{ K}$

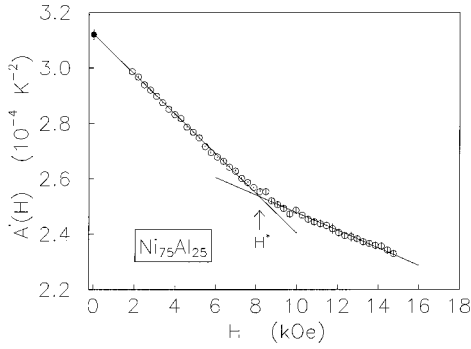


FIG. 6. Field dependence of the coefficient  $A'(H)$  of the  $T^2$  term appearing in Eq. (32) of the text. The straight lines through the data (open circles) represent the least-squares fits based on Eq. (35) of the text. Upward arrow indicates the field  $H^*$  at which an abrupt change in the slope occurs. Note that the vertical error bars are of the size of the data symbols wherever they are not specified but the horizontal error bars are extremely small ( $\pm 1$  Oe) compared to the data symbol size. Notice that the straight line for fields  $H \leq H^*$ , when extrapolated to  $H=0$ , yields a value for  $A'$  at  $H=0$  that is equal to the value  $A'(H=0) = 3.12(2) \times 10^{-4} \text{ K}^{-2}$  (closed circle) which is directly determined from the spontaneous magnetization data.

( $\approx 0.5T_C$ ), as is evident from the typical percentage deviation plot shown in the lower part of Fig. 5(a). (II) The lower and upper limits of the temperature range over which Eq. (32) completely accounts for the observed temperature dependence of  $M$  do not exhibit any systematic variation with  $H$ . (III) Since, irrespective of the value of  $H$ , a strong correlation was observed in the values of the coefficients  $A'$  and  $A''$  when all the three parameters  $M(0,H)$ ,  $A'$ , and  $A''$  were varied to arrive at the optimum fit to the data based on Eq. (32),  $A''$  (or  $A'$ ) was kept fixed at a given value while the remaining two parameters were optimized. This procedure was repeated for other fixed values of  $A''$  (or  $A'$ ) until a global minimum in the sum of the deviation squares was obtained. Such a fitting method unambiguously demonstrates that  $A'' = 7.27(3) \times 10^{-4} \text{ K}^{-4/3}$  for the values of  $H$  ranging between 0 and 14.75 kOe whereas  $A'$  varies with  $H$  as shown in Fig. 6. A linear relation between  $A'$  and  $H$  of the type

$$A'(H) = A'(H=0)(1 - \alpha H) \quad (35)$$

and an abrupt change in slope ( $\equiv \alpha$ ) at  $H^* \approx 8$  kOe is evident from this figure. The least-squares fits, based on Eq. (35), attempted to the  $A'(H)$  data and shown in Fig. 6 by the straight lines yield the values of the slope as  $\alpha = 2.12(13) \times 10^{-5} \text{ Oe}^{-1}$  and  $\alpha = 1.05(10) \times 10^{-5} \text{ Oe}^{-1}$  in the field ranges  $0 \leq H \leq 8$  kOe and  $8 \leq H \leq 14.75$  kOe, respectively. A linear field dependence of the coefficient of the  $T^2$  term [in the expression for  $M(T,H)$ ] of the form Eq. (35) has also been previously observed<sup>34</sup> in fcc Fe-Ni Invar alloys with Ni concentration in at. % as 34.2, 35.4, and 37.0 in the intermediate temperature range. These alloys too exhibit weak itinerant-electron ferromagnetism. While the present value of  $A'(H=0) = 3.12(2) \times 10^{-4} \text{ K}^{-2}$  (Fig. 6) compares well with the previously reported<sup>1,2</sup> value of  $3.92 \times 10^{-4} \text{ K}^{-2}$  for ordered  $\text{Ni}_3\text{Al}$ , the coefficient (slope)  $\alpha$  for  $H \geq 8$  kOe, in

the present case, possesses a value that is exactly one order of magnitude larger than that [ $\alpha = 1.2(2) \times 10^{-6} \text{ Oe}^{-1}$ ] determined earlier<sup>34</sup> for fcc Fe-Ni weak itinerant-electron ferromagnets in the field range  $8 \leq H \leq 52.7$  kOe. In conformity with the predictions of the MSF model,<sup>28</sup> at intermediate temperatures, the thermally excited spin fluctuations, which manifest themselves as the  $T^2$  term in Eqs. (22) or (32), dominantly contribute to the thermal demagnetization of  $M(T,0)$  and  $M(T,H)$  and get strongly suppressed by magnetic field [Eq. (35) and Fig. 6] whereas the zero-point spin fluctuations which are mainly responsible for the  $T^{4/3}$  term in Eqs. (22) or (32), make a significant contribution to the decline of  $M(T,0)$  and  $M(T,H)$  with increasing temperature and are not affected by the field. However, this model, like the conventional spin-fluctuation theories, does not offer any explanation for the linear field dependence of  $A'$  and an abrupt decrease (by a factor of 2) in the value of slope  $\alpha$  at  $H^* \approx 8$  kOe.

For temperatures below  $T_C$  but just outside the critical region ( $T \lesssim T_C$ ), the following observations have been made based on the range-of-fit analysis of the magnetization data in terms of the expressions given by Eqs. (21a), (21b), (26), and (30)–(34). The observed temperature variation of spontaneous magnetization as well as in-field magnetization at such temperatures is best described by Eqs. (26), (33), or (34), as is clearly noticed not only from the percentage deviation plot displayed in the bottom part of Fig. 7(a) (which is representative of similar plots at other values of  $H$ , including  $H=0$ , as well) but also from the data presented in Fig. 7(b). The temperature range over which  $M^2(T,H)$  or  $M^2(T,0)$  varies with temperature as  $T^{4/3}$  broadens while the slope  $A(H)$  of the  $M^2(T,H)$  versus  $T^{4/3}$  straight lines [cf. Eqs. (34) and (26)] decreases as  $H$  increases. The variation of the coefficient  $A(H)$  of the  $T^{4/3}$  term in Eqs. (26) or (34) with  $H$  is depicted in Fig. 8 wherein  $A$  is plotted against  $H$  and  $H^{1/2}$ . Figure 8 demonstrates that the  $A(H)$  data obey Eq. (27) to a very high degree of accuracy and that the best least-squares fit to the  $A(H)$  and  $A(\sqrt{H})$  data based on Eq. (27), represented by the continuous curve and straight line, respectively, yield exactly the same value of  $A(H=0)$  upon extrapolation to  $H=0$  as that obtained directly from the  $M^2(T,0)$  versus  $T^{4/3}$  plot [Fig. 7(c)]. According to the MSF model,<sup>28</sup> the terms  $T^2$  and  $T^{4/3}$  in Eq. (26) originate from Stoner single-particle excitations and thermally-excited (TE) plus zero-point (ZP) spin fluctuations, respectively, and that the TE spin-fluctuation contribution to the coefficient  $A(H=0)$  dominates over that arising from ZP spin fluctuations in the temperature range in question (Sec. II). In view of this genesis of the  $T^2$  and  $T^{4/3}$  terms, the experimental observation that the percentage deviation has the *same* value [Fig. 7(a)] for the fits that either include [Eq. (26)] or exclude [Eq. (34)] the  $T^2$  term asserts that the overwhelmingly large spin-fluctuation contribution completely swamps the feeble contribution to  $M(T,0)$  or  $M(T,H)$  arising from Stoner single-particle excitations. The relative importance of spin fluctuations and single-particle excitations could not be ascertained at intermediate temperatures because in this temperature regime, both the types of excitations, give contributions to  $M(T,0)$  and  $M(T,H)$  that vary with temperature as

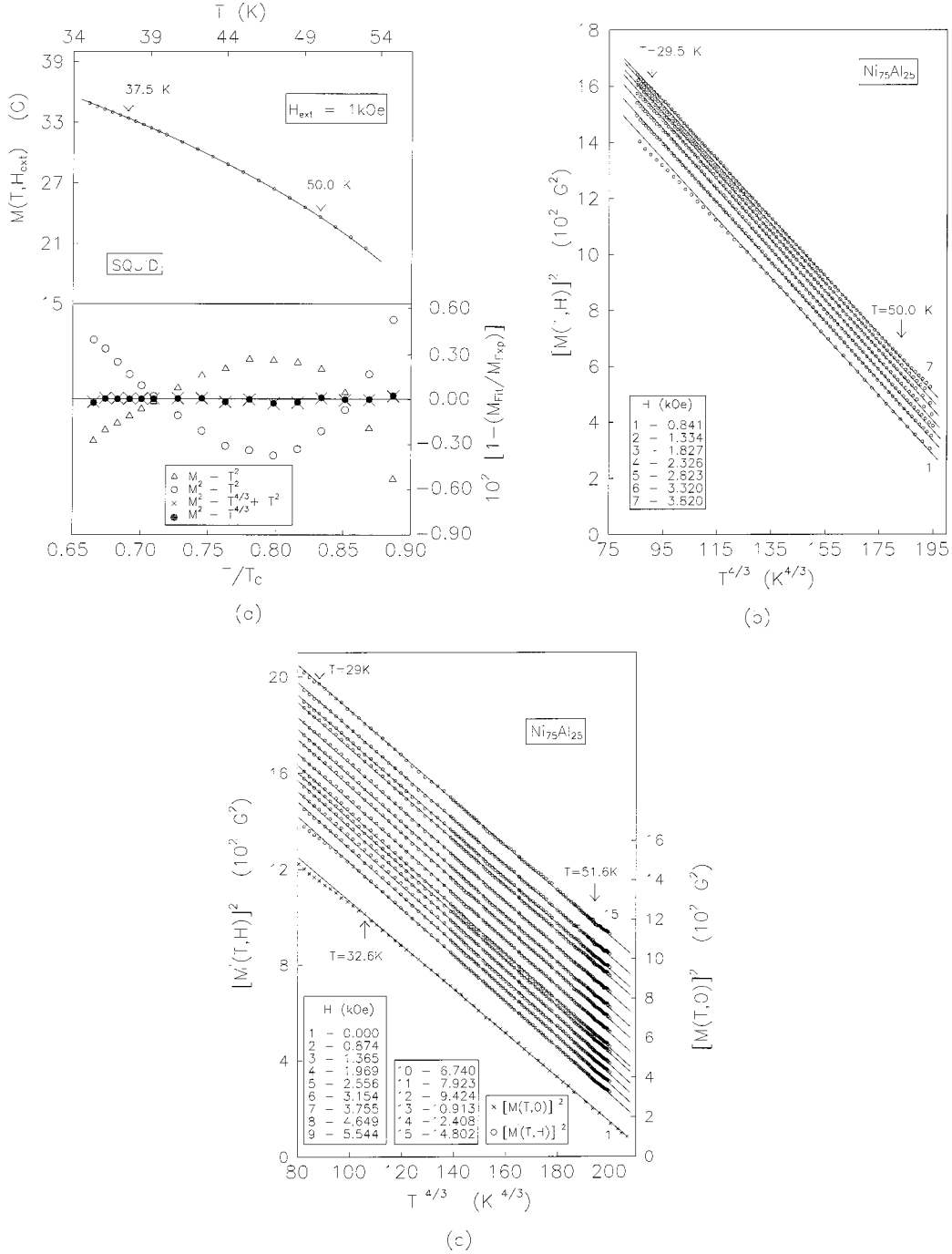


FIG. 7. Temperature variation of in-field magnetization, (a)  $M(T, H_{ext} = 1$  kOe), (b)  $M(T, H)$ , and (c)  $M'(T, H)$ , at a few selected but fixed values of  $H$  for temperatures in the range  $28 \leq T \leq 54$  K. Part (c) of the figure, in addition, depicts the temperature dependence of spontaneous magnetization in this temperature range. The continuous curve and straight lines represent the best least-squares fits to the  $M(T, H)$  data (open circles) and  $M(T, 0)$  data (crosses) based on Eq. (34) of the text. The lower panel of Fig. 7(a) displays the percentage deviation of the  $M(T, H_{ext} = 1$  kOe) SQUID data from the fits based on Eq. (30) (open triangles), Eq. (31) (open circles), Eq. (26) (crosses), and Eq. (34) (closed circles) of the text.

$T^2$  [Eqs. (22) and (23)]. That Stoner single-particle excitations decrease magnetization with increasing temperature at a rate which is extremely slow compared to that due to spin fluctuations has also been previously inferred<sup>18,22</sup> from band-structure calculations and the results of de Haas-Van Alphen effect measurements on Ni<sub>3</sub>Al. The observation that  $A(H) \sim H^{1/2}$  for fields in the range  $0 \leq H \leq 15$  kOe was previously made by us<sup>31,35</sup> on amorphous weak itinerant-electron ferromagnets as well. Thus Eq. (27) quantifies the suppression of

thermally excited spin fluctuations [since they are solely responsible for the  $H^{1/2}$  term in Eq. (27); see Sec. II] at weak and intermediate fields in weak itinerant-electron ferromagnets regardless of whether they are crystalline or amorphous and unlike the previous expression,<sup>20,36</sup> based on the electron-gas model, involves only a *single* fitting parameter  $\eta$  because the value of  $A(H=0)$  can be obtained directly from the spontaneous magnetization data. Moreover, the presently determined value of  $A(H=0) = 4.65(3) \times 10^{-3} \text{ K}^{-4/3}$  yields

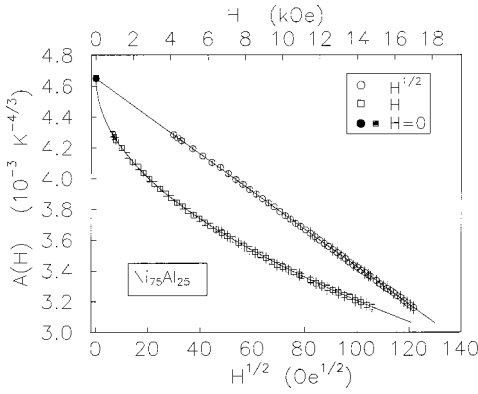


FIG. 8. Field dependence of the coefficient  $A(H)$  of the  $T^{4/3}$  term appearing in Eq. (34) of the text. The continuous curve or the straight line represents the least-squares fit to the  $A(H)$  data (open squares) or  $A(\sqrt{H})$  data (open circles) based on Eq. (27) of the text. Notice that these fits, when extrapolated to  $H=0$ , yield a value for  $A$  at  $H=0$  that exactly coincides with that  $[A(H=0)=4.65(3) \times 10^{-3} \text{ K}^{-4/3}]$  (closed circle or square) directly determined from the spontaneous magnetization data. Note that the vertical error bars are of the size of the data symbols wherever they are not specified but the horizontal error bars are extremely small ( $\pm 1$  Oe) compared to the data symbol size.

the value for the Curie temperature as  $T_C^{SF} = 56.2(3)$  K when the relation  $T_C^{SF} = [A(H=0)]^{-3/4}$  [Eq. (28)] is used. This value is quite close to the value  $T_C = 56.45(5)$  K obtained from the Arrott plot (Fig. 2). This finding implies that, barring the low-temperature region [where spin waves govern  $M(T,0)$ ], the temperature dependence of spontaneous magnetization is primarily determined by the enhanced spin-density fluctuations and that Stoner single-particle excitations have a negligible role to play in  $M(T,0)$  of  $\text{Ni}_3\text{Al}$ .

Finally, as shown below, the present results facilitate the rationalization of the previous seemingly contradictory notions about the nature of low-lying magnetic excitations in  $\text{Ni}_3\text{Al}$  based on distinctly different temperature variations observed for spontaneous magnetization in the same or similar temperature ranges and the results of SANS and INS experiments (for details, see Introduction). Our results demonstrate that the relations  $M(T,0) = M(0,0) - aT^2$  and  $M^2(T,0) = M^2(0,0) - a'T^2$  describe the magnetization data equally well even though the data present systematic deviations of roughly the same magnitude from the fits based on both these relations [Figs. 4 and 5(a)] and that far greater precision in the measurement of magnetization than achieved hitherto is required to establish the actual functional form of  $M(T,0)$  and  $M(T,H)$  in different temperature ranges, and hence the exact nature of magnetic excitations that dominate in those temperature regions. Next, we address ourselves to the apparent discrepancy between the results of previous SANS and INS experiments and those of the present magnetization measurements. To elucidate this point further, in sharp contrast with the claim made by Bernhoeft and co-workers<sup>24,25</sup> that spin-wave excitations completely account for the temperature dependence of SANS and INS intensity in the temperature range  $0.1T_C \leq T \leq 0.8T_C$ , the results of present investigation show that spin waves enjoy overwhelming presence only for temperatures in the range  $0.09T_C \leq T \leq 0.28T_C$  and are completely overshadowed by

nonpropagating spin fluctuations for temperatures ranging from  $0.32T_C$  to  $0.92T_C$ . Recognizing the fact that nonpropagating spin fluctuations show up as a central elastic peak at  $\Delta E = 0$  whereas spin waves give rise to peaks at  $\Delta E \neq 0$  in the constant- $q$  INS spectra taken at different temperatures, spin fluctuations can easily evade detection in such spectra if the instrumental resolution is not high enough, which seems to be the case with the reported<sup>25</sup> INS spectra.

## V. SUMMARY AND CONCLUSION

Extensive high-resolution magnetization,  $M(T, H_{ext})$ , measurements were performed on well-characterized  $\text{Ni}_3\text{Al}$  polycrystalline sample at temperatures in the range  $14 \leq T \leq 80$  K ( $5 \leq T \leq 100$  K) in fields up to 15 kOe (at  $H_{ext} = 1$  kOe) as well as at 5 K in fields up to 70 kOe. We obtain the values for the spontaneous magnetization at 5 K,  $M(T=5 \text{ K}, 0) = 46.75(12)$  G or magnetic moment per Ni atom =  $0.0766(2)\mu_B/\text{Ni}$  atom, the zero-field differential susceptibility at 5 K,  $\chi(T=5 \text{ K}, 0) = 3.56(30) \times 10^{-4}$  and the Curie temperature  $T_C = 56.45(5)$  K. While the values of  $M(T=5 \text{ K}, 0)$  and  $\chi(T=5 \text{ K}, 0)$  are in excellent agreement with those reported<sup>1,2,10,11</sup> previously for ordered  $\text{Ni}_3\text{Al}$ , the value of  $T_C$  is substantially higher than the published<sup>1,2,10,11</sup> value  $T_C = 41(1)$  K.

An elaborate range-of-fit analysis of the in-field magnetization  $M(T, H)$  and spontaneous magnetization  $M(T, 0)$  data based on the expressions for these quantities given by the recent theoretical calculations<sup>27,28</sup> in different temperature ranges reveals the following.

(i) Spin-wave excitations almost entirely account for the observed thermal demagnetization of spontaneous as well as in-field magnetization at low temperatures  $T \leq 0.28T_C$ . Spin-wave stiffness possesses a field-independent value of  $69.6(14) \text{ meV \AA}^2$  which conforms well with the values directly determined from small-angle neutron-scattering and inelastic neutron-scattering experiments previously.

(ii) Enhanced fluctuations in local magnetization manifest themselves in  $M(T, 0)$  and  $M(T, H)$  through a contribution that varies with temperature as  $M(T, H) = M(0, H)[1 - A'(H)T^2 - A''T^{4/3}]^{1/2}$  and  $M(T, H) = M(0, H)[1 - A(H)T^{4/3}]^{1/2}$  for temperatures in the ranges  $0.32T_C \leq T \leq 0.50T_C$  and  $0.51T_C \leq T \leq 0.92T_C$ , respectively. At these temperatures ( $0.32T_C \leq T \leq 0.92T_C$ ), this contribution to  $M(T, 0)$  and  $M(T, H)$  completely overshadows the one arising from spin waves. The coefficient  $A''$  does not depend on  $H$  while the coefficients  $A'(H)$  and  $A(H)$  vary with  $H$  in accordance with the relations  $A'(H) = A(H=0)(1 - \alpha H)$  and  $A(H) = A(H=0)(1 - \eta\sqrt{H})$ . An abrupt change in the value of the slope  $\alpha$  is observed at  $H^* \approx 8$  kOe. These relations quantify the suppression of thermally excited (TE) spin fluctuations by magnetic field whereas magnetic field has little, or even no, influence on zero-point (ZP) spin fluctuations. Of the two components ZP and TE of spin fluctuations, TE spin fluctuations basically dictate the temperature dependence of  $M(T, 0)$  and  $M(T, H)$  at intermediate temperatures and for temperatures just outside the critical region but below  $T_C$ .

(iii) Stoner single-particle excitations make a negligibly small contribution to the temperature variation of spontaneous and in-field magnetization.

(iv) All the observations (i)–(iii) stated above, except for the linear relationship between  $A'$  and  $H$  as well as the abrupt change in  $\alpha$  at  $H^* \approx 8$  kOe, testify to the validity of the theoretical predictions based on the so-called modified spin-fluctuation model.<sup>27,28</sup>

## ACKNOWLEDGMENTS

The authors are grateful to Professor H. Kronmüller for permitting the use of SQUID magnetometer and to A. Meyer for the chemical analysis of the Ni<sub>3</sub>Al samples. This work was supported by the Department of Science and Technology, India, under Grant D.O.No. SP/S2/M-21/97. One of the authors (A.S.) is grateful to the Council of Scientific and Industrial Research, India, for financial support.

\*Electronic address: kaulsp@uohyd.ernet.in

- <sup>1</sup>F.R. de Boer, C.J. Schinkel, J. Biesterbos, and S. Proost, *J. Appl. Phys.* **40**, 1049 (1969).
- <sup>2</sup>P.F. De Chatel and F.R. De Boer, *Physica (Amsterdam)* **48**, 331 (1970).
- <sup>3</sup>C.G. Robbins and H. Claus, in *Proceedings of the 17th Annual Conference on Magnetism and Magnetic Materials*, edited by C. D. Graham, Jr., G. H. Lander, and J. J. Rhyne, AIP Conf. Proc. No. 24 (AIP, New York, 1972), p. 527.
- <sup>4</sup>C.J. Shinkel, F.R. de Boer, and B. de Hon, *J. Phys. F* **3**, 1463 (1973).
- <sup>5</sup>T.F.M. Kortekaas and J.J.M. Franse, *J. Phys. F* **6**, 1161 (1976).
- <sup>6</sup>J.J.M. Franse, *Physica B & C* **86-88B**, 283 (1977); E.P. Wohlfarth, *ibid.* **91B**, 305 (1977).
- <sup>7</sup>N. Buis, J.J.M. Franse, and P.E. Brommer, *Physica B & C* **106B**, 1 (1981).
- <sup>8</sup>J.J.M. Buiting, J. Kübler, and F.M. Mueller, *J. Phys. F* **13**, L179 (1983).
- <sup>9</sup>T. Umemura and Y. Masuda, *J. Phys. Soc. Jpn.* **52**, 1439 (1983).
- <sup>10</sup>H. Sasakura, K. Suzuki, and Y. Masuda, *J. Phys. Soc. Jpn.* **53**, 352 (1984); **53**, 754 (1984).
- <sup>11</sup>S. Takahashi, A.Y. Takahashi, and A. Chiba, *J. Phys.: Condens. Matter* **6**, 6011 (1994).
- <sup>12</sup>E.C. Stoner, *Proc. R. Soc. London, Ser. A* **139**, 339 (1939).
- <sup>13</sup>E.P. Wohlfarth, *Rev. Mod. Phys.* **25**, 211 (1953); D.M. Edwards and E.P. Wohlfarth, *Proc. R. Soc. London, Ser. A* **303**, 127 (1968).
- <sup>14</sup>T. Moriya and A. Kawabata, *J. Phys. Soc. Jpn.* **34**, 639 (1973); **35**, 669 (1973); A. Kawabata, *J. Phys. F* **4**, 1477 (1974).
- <sup>15</sup>T.V. Ramakrishnan, *Solid State Commun.* **14**, 449 (1974); *Phys. Rev. B* **10**, 4014 (1974).
- <sup>16</sup>S.G. Mishra and T.V. Ramakrishnan, *J. Phys. C* **10**, L667 (1977); *Phys. Rev. B* **18**, 2308 (1978).
- <sup>17</sup>T. Moriya and Y. Takahashi, *J. Phys. Soc. Jpn.* **45**, 397 (1978).
- <sup>18</sup>G.G. Lonzarich, *J. Magn. Magn. Mater.* **45**, 43 (1984); G.G. Lonzarich and L. Taillefer, *J. Phys. C* **18**, 4339 (1985).
- <sup>19</sup>Y. Takahashi and T. Moriya, *J. Phys. Soc. Jpn.* **54**, 1592 (1985).
- <sup>20</sup>T. Moriya, in *Spin Fluctuations in Itinerant Electron Magnetism*, edited by P. Fulde, Springer Series in Solid State Sciences Vol. 56 (Springer, Berlin, 1985).
- <sup>21</sup>Y. Takahashi, *J. Phys. Soc. Jpn.* **55**, 3553 (1986).
- <sup>22</sup>G.G. Lonzarich, *J. Magn. Magn. Mater.* **54-57**, 612 (1986).
- <sup>23</sup>S.G. Mishra, *Mod. Phys. Lett. B* **4**, 83 (1990).
- <sup>24</sup>N.R. Bernhoeft, I. Cole, G.G. Lonzarich, and G.L. Squires, *J. Appl. Phys.* **53**, 8204 (1982).
- <sup>25</sup>N.R. Bernhoeft, G.G. Lonzarich, P.W. Mitchell, and D. McK. Paul, *Phys. Rev. B* **28**, 422 (1983).
- <sup>26</sup>C. Herring and C. Kittel, *Phys. Rev.* **81**, 869 (1951); C. Herring, *ibid.* **85**, 1003 (1952); **87**, 60 (1952); *Proc. R. Soc. London, Ser. A* **371**, 67 (1980).
- <sup>27</sup>S.N. Kaul and A. Semwal, *Phys. Lett. A* **254**, 101 (1999).
- <sup>28</sup>S.N. Kaul, *J. Phys.: Condens. Matter* **11**, 7597 (1999).
- <sup>29</sup>W. Grant, *J. Met.* **9**, 865 (1957).
- <sup>30</sup>K. Aoki and O. Izumi, *Phys. Status Solidi A* **32**, 657 (1975), and references cited therein.
- <sup>31</sup>S.N. Kaul and P.D. Babu, *J. Phys.: Condens. Matter* **10**, 1563 (1998).
- <sup>32</sup>S.N. Kaul, *J. Phys.: Condens. Matter* **3**, 4027 (1991); S.N. Kaul and P.D. Babu, *ibid.* **4**, 6429 (1992).
- <sup>33</sup>S.N. Kaul and P.D. Babu, *Phys. Rev. B* **50**, 9308 (1994).
- <sup>34</sup>I. Nakai and H. Maruyama, *J. Magn. Magn. Mater.* **104-107**, 2053 (1992); I. Nakai, *J. Phys. Soc. Jpn.* **59**, 2211 (1990).
- <sup>35</sup>P.D. Babu and S.N. Kaul, *J. Phys.: Condens. Matter* **9**, 3625 (1997).
- <sup>36</sup>J. Takeuchi and Y. Masuda, *J. Phys. Soc. Jpn.* **46**, 468 (1979).